Transcriptome analysis of *Valsa mali* reveals its response mechanism to the biocontrol actinomycete *Saccharothrix yanglingensis* Hhs.015

Cong Liu [1, 2], **Dongying Fan** [1, 2], **Yanfang Li** [1, 2], **Yue Chen** [1, 2], **Lili Huang** [Corresp., 1, 3], **Xia Yan** [Corresp. 1, 2]

[1] State Key Laboratory of Crop Stress Biology for Arid Areas, Northwest A&F University, Yangling, Shaanxi, China

[2] College of Life Science, Northwest A&F University, Yangling, Shaanxi, China

[3] College of Plant Protection, Northwest A&F University, Yangling, Shaanxi, China

Corresponding Authors: Lili Huang, Xia Yan
Email address: huanglili@nwsuaf.edu.cn, yanxia@nwsuaf.edu.cn

Apple canker is a devastating branch disease caused by *Valsa mali* (*Vm*). The endophytic actinomycete *Saccharothrix yanglingensis* Hhs.015 (*Sy* Hhs.015) can effectively inhibit the growth of *Vm*. To reveal the mechanism, by which *Vm* respond to *Sy* Hhs.015, the transcriptome of *Vm* was analyzed using RNA-seq technology. Compared with the control group, 1476 genes were significantly differentially expressed in the treatment group, of which 851 genes were up-regulated and 625 genes were down-regulated. Combined gene function and pathway analysis of differentially expressed genes (DEGs) revealed that *Sy* Hhs.015 affected the carbohydrate metabolic pathway, which is utilized by *Vm* for energy production. Approximately 82% of the glycoside hydrolase genes were down-regulated, including three pectinase genes (PGs), which are key pathogenic factors. The cell wall structure of *Vm* was disrupted by *Sy* Hhs.015 and cell wall-related genes were found to be down-regulated. Of the peroxisome associated genes, those encoding catalase (CAT) and superoxide dismutase (SOD) which scavenge reactive oxygen species (ROS), as well as those encoding AMACR and ACAA1 which are related to the β-oxidation of fatty acids, were down-regulated. MS and ICL, key genes in glyoxylate cycle, were also down-regulated. In response to the stress of *Sy* Hhs.015 exposure, *Vm* increased amino acid metabolism to synthesize the required nitrogenous compounds, while alpha-keto acids, which involved in the TCA cycle, could be used to produce energy by deamination or transamination. Retinol dehydrogenase, associated with cell wall dextran synthesis, and sterol 24-C-methyltransferase, related to cell membrane ergosterol synthesis, were up-regulated. The genes encoding glutathione S-transferase, (GST), which has antioxidant activity and ABC transporters which have an efflux function, were also up-regulated. These results show that the response of *Vm* to *Sy* Hhs.015 exposure is a complicated and highly regulated process, and provide a theoretical basis for both clarifying the biocontrol mechanism of *Sy*

Hhs.015 and the response of *Vm* to stress.

Transcriptome analysis of *Valsa mali* reveals its response mechanism to the biocontrol actinomycete *Saccharothrix yanglingensis* Hhs.015

Cong Liu[1,2], Dongying Fan[1,2], Yanfang Li[1,2], Yue Chen[1,2], Lili Huang[1,3], Xia Yan[1,2]

[1] State Key Laboratory of Crop Stress Biology for Arid Areas, Northwest A&F University, Yangling, Shaanxi, China
[2] College of Life Science, Northwest A&F University, Yangling, Shaanxi, China
[3] College of Plant Protection, Northwest A&F University, Yangling, Shaanxi, China

Corresponding Author：

Xia Yan[1,2]
Email address: yanxia@nwsuaf.edu.cn

Lili Huang[1,3]
Email address: huanglili@nwsuaf.edu.cn

Abstract

Apple canker is a devastating branch disease caused by *Valsa mali* (*Vm*). The endophytic actinomycete *Saccharothrix yanglingensis* Hhs.015 (*Sy* Hhs.015) can effectively inhibit the growth of *Vm*. To reveal the mechanism, by which *Vm* respond to *Sy* Hhs.015, the transcriptome of *Vm* was analyzed using RNA-seq technology. Compared with the control group, 1476 genes were significantly differentially expressed in the treatment group, of which 851 genes were up-regulated and 625 genes were down-regulated. Combined gene function and pathway analysis of differentially expressed genes (DEGs) revealed that *Sy* Hhs.015 affected the carbohydrate metabolic pathway, which is utilized by *Vm* for energy production. Approximately 82% of the glycoside hydrolase genes were down-regulated, including three pectinase genes (PGs), which are key pathogenic factors. The cell wall structure of *Vm* was disrupted by *Sy* Hhs.015 and cell wall-related genes were found to be down-regulated. Of the peroxisome associated genes, those encoding catalase (CAT) and superoxide dismutase (SOD) which scavenge reactive oxygen species (ROS), as well as those encoding AMACR and ACAA1 which are related to the β-oxidation of fatty acids, were down-regulated. MS and ICL, key genes in glyoxylate cycle, were also down-regulated. In response to the stress of *Sy* Hhs.015 exposure, *Vm* increased amino acid metabolism to synthesize the required nitrogenous compounds, while alpha-keto acids, which involved in the TCA cycle, could be used to produce energy by deamination or transamination. Retinol dehydrogenase, associated with cell wall dextran synthesis, and sterol 24-C-methyltransferase, related to cell membrane ergosterol synthesis, were up-regulated. The genes encoding glutathione S-transferase, (GST), which has antioxidant activity and ABC transporters which have an efflux function, were also up-regulated. These results show that the response of *Vm* to *Sy* Hhs.015 exposure is a complicated and highly regulated process, and provide a theoretical basis for both clarifying the biocontrol mechanism of *Sy* Hhs.015 and the response of *Vm* to stress.

Introduction

Apple canker is a serious and potentially devastating branch disease caused by the ascomycetous fungus, *Valsa mali* (*Vm*), which occurs in the main apple producing areas of China (Cao et al., 2009; Wang et al., 2014b), and causes serious economic losses. Currently, chemical treatment methods, such as scraping the canker lesion and applying fungicides, are the main strategies for preventing and treating apple canker (Li et al., 2016). However, large quantities of chemicals pollute the environment and can easily lead to drug-resistant pathogens. The usage of biological control agents has drawn increasing attention because they are environmentally friendly, long-term and continuous (Compant et al., 2005; Miles et al., 2012).

Vm is a weak parasitic fungus that usually infects wounded or necrotic branches rather than healthy ones. *Vm* also has latent infection characteristics, as observed from the fact that decomposition of apple branches that look apparently free from disease can occur after specific treatments (Biggs 1990). The process of *Vm* infecting apple trees is complicated, and cell wall-degrading enzymes, secondary metabolites, and effector proteins might play important roles in

their pathogenic mechanism (Yin et al., 2015). During the process of infecting apple bark, the expression of genes related to catabolism, hydrolase activity and secondary metabolite biosynthesis are up-regulated (Ke et al., 2014). Additionally, the use of immunocytochemistry labeling has shown that pectinases play an important role in the infection process (Ke et al., 2014). *Vm* can also produce toxins such as protocatechuic acid, p-hydroxybenzoic acid, p-hydroxyacetophenone, 3-p-hydroxyphenylpropionic acid and phloroglucinol (Wang et al., 2014a). Several toxin-associated genes have been identified in the genome of *Vm*, and genes related to secondary metabolism such as cytochrome P450, non-ribosomal polypeptide synthetase and monooxygenase, have been shown to be up-regulated during infection (Yin et al., 2015).

Actinomycetes are a class of microbes that are kown to produce bioactive substances (Qin et al., 2011). They are of potential value to biocontrol because they can inhibit pathogens by producing natural products such as antibiotics and extracellular enzymes (Castillo et al., 2002). The *Saccharothrix yanglingensis* strain Hhs.015 (*Sy* Hhs.015) is an endophytic actinomycete isolated from the root of cucumber (Yan et al., 2012). Both laboratory and field experiments have proven that *Sy* Hhs.015 is a good inhibitor of apple canker. In vitro experiments has shown that *Sy* Hhs.015 sterile fermentation filtrate can inhibit the growth of mycelium and conidia germination of *Vm*, and abnormal mycelia and cytoplasmic extravasation can be observed. Field experiments has shown that the relative control efficiency of apple trees infected with *Vm* after *Sy* Hhs.015 treatment was 61.29%, which was equivalent to that of treatment with difenoconazole and tebuconazole (Fan et al., 2016). Studies have shown that *Sy* Hhs.015 can produce heteroauxin, chitinase, proteinase and glucanase, and the active substances isoflavones and pentamycin have been extracted from its fermentation broth (Fan et al., 2016).

This study aims to elucidate why *Vm* is inhibited by *Sy* Hhs.015, and the mechanism of its response to *Sy* Hhs.015 stress, by using RNA-seq to compare the expression of *Vm* in its normal growth state to the expression of *Vm* under the inhibition of *Sy* Hhs.015.

Materials & Methods

Strains and culture conditions

Saccharothrix yanglingensis strain Hhs.015 and *Valsa mali* virulent strain 03-8, were provided by the Laboratory of Integrated Management of Plant Diseases, College of Plant Protection, Northwest A&F University, Yangling, Shaanxi Province, China and sorted at -80 °C.

Vm 03-8, on potato dextrose agar (PDA) and incubated at 25 °C for 3 days. *Sy* Hhs.015 was cultured on Gause's No.1 synthetic agar medium and incubated at 28 °C for 7 days in the dark to induce sufficient sporulation.

V. mali/*S. yanglingensis* confrontation assay

A section of agar 0.5 cm in width and 8.5 cm in length was taken from a plate of Gaose's No.1 agar previously inoculated with *Sy* Hhs.015 and placed on the middle of a fresh PDA plate covered with sterile cellophane. Another section of agar 0.5 cm in width and 7.0 cm in length was taken from a plate of PDA inoculated with *Vm* and placed on the new PDA plate, 2 cm from *Sy*

Hhs.015 agar strip (Fig. 1). After culture at 25 °C for 48 hours in the dark, the mycelia at the *Sy* Hhs.015-exposed boundary of the *Vm* culture were collected and labeled as the treatment group. As a control, mycelia were collected from unexposed *Vm*. The experimental sample had three biological replicates. Samples were lyophilized with liquid nitrogen and stored at -80 °C.

RNA extraction and sequencing

Total RNA of the samples was extracted using the RNeasy Micro kit (Qiagen, Shenzhen, PRC). RNA degradation and contamination of the samples were assessed on 1% agarose gels. RNA purity was analyzed using a NanoPhotometer® spectrophotometer (IMPLEN, CA, USA). RNA concentration was measured using the Qubit® RNA Assay Kit in a Qubit® 2.0 Fluorometer (Life Technologies, CA, USA). RNA integrity was assessed using the RNA Nano 6000 Assay Kit of the Agilent Bioanalyzer 2100 system (Agilent Technologies, CA, USA).

A total of 3 μg of RNA per sample was used as input material for the RNA sample preparations. Sequencing libraries were generated using NEBNext® Ultra™ RNA Library Prep Kit for Illumina® (NEB, USA) following manufacturer's recommendations and index codes were added to attribute sequences to each sample. The library preparations were sequenced on an Illumina Hiseq 2000 platform, where 125bp paired-end reads were generated.

Raw read cleaning, mapping to reference genome, and gene annotation

Trimmomatic (Version 0.36) was applied to obtain high-quality clean reads by trimming and filtering raw reads (BolgerLohse & Usadel 2014). The clean data for each sample was mapped to the *Vm* reference genome (NCBI ACCESSION: JUIY00000000) using default parameters of HISAT2 (Version 2.1.0) (KimLangmead & Salzberg 2015). Using HTseq-count (Version 0.8.0), the number of reads mapped to each gene was calculated based on the SAM / BAM alignment result file and the GTF file of the gene structure to obtain a count matrix for differential expression analysis (AndersPyl & Huber 2015).

Blastp (2.4.0, E-value < 1e-5) was used to align all genes with Nr, KOG, KEGG databases for functional annotation. The GO (Gene Ontology) annotation of the genes were obtained using Blast2GO (version 4.1) software (Conesa et al., 2005).

Differential expression analysis, GO, and KEGG enrichment analysis

Differentially expressed genes were identified between the *Vm* samples that were inhibited by *Sy* Hhs.015, and untreated *Vm* samples using R-package DESeq2 (Version 1.10.1) (LoveHuber & Anders 2014). The package DESeq2 provides methods to test differential expression by using negative binomial generalized linear models. Log2-fold change, p-value and adjusted p-value were calculated for all genes. Genes with a $|\log2FC| \geq 1$ and $P.adj < 0.05$ were considered to be differentially expressed genes (DEGs).

Using GO and KEGG annotations of all genes in the *Vm* genome as background, GO and KEGG pathway enrichment analysis of DEGs was performed using a hypergeometric distribution test (Subramanian et al., 2005).

Quantitative reverse transcription-PCR (qRT-PCR)

To confirm the reliability of DEGs, 10 genes were selected for qRT-PCR validation, while the endogenous gene glucose-6-phosphate-dehydrogenase (G6PDH) was used as a control. Primer Premier (Version 5.0) was used to design primers for the 10 selected DEGs (Table 1). PCR amplification was performed using the BIO-RAD system and the expression analysis was carried out using built-in software. The reaction system consisted of 1 μL of cDNA, 0.5 μL of 10 μM PCR primer, SYBR Premix ExTaq (1x, 10 μL; TaKaRa Bio Inc.) as a total of 20 μL. PCR program was as follows: 95 °C for 1 min, 40 cycles (95 °C for 15 s, 55 °C for 20 s, and 72 °C for 45 s). A dissolution curve was then generated. The qPCR for each gene was repeated 3 times, and the average (Ct) was calculated. The relative expression level of each gene was calculated using the $2^{-\Delta\Delta Ct}$ method.

Results

Inhibition of *Vm* by *Sy* Hhs.015

The *V. mali*/*S. yanglingensis* confrontation assay showed that at 48 h *Sy* Hhs.015 significantly inhibited the growth of *Vm* mycelia (Fig. 2A and 2B). Additionally, quantities of abnormal mycelia could be observed using an optical microscope (Fig. 2C and 2D). Transmission electron microscopy of the subcellular structure of abnormal mycelia showed that the cell wall had thickened, almost all the cytoplasm had degenerated completely and a large vacuole had formed. In addition, the nucleus had fully separated from the cytoplasm, while several cells had even completely degraded in the nucleus (Fig. 2E and 2F).

Sequencing quality control, quantification of gene expression levels, and annotation of gene function

The total number of raw reads obtained by sequencing was 133185208, while the total number of clean reads after filtration was 126932206. The total number of clean reads bases was 15.86 Gb. The error rate of each sample was less than 0.04%, Q20 was greater than 94.24%, Q30 was greater than 89.06%, and GC content was 55.02%-55.84%. The raw data of all samples (three controls and three treatments) reported in this study have been deposited in the Genome Sequence Archive (Genomics, Proteomics & Bioinformatics 2017) in BIG Data Center (Nucleic Acids Res 2018), Beijing Institute of Genomics (BIG), Chinese Academy of Sciences, under accession number CRA000693, which is publicly accessible at http://bigd.big.ac.cn/gsa. Sequencing data showed that quality and accuracy were both excellent (Table 2). The mapping rate of each sample was higher than 96.4%. The count matrix for each sample was also obtained (Table S1).

KOG (Eukaryotic Ortholog Groups) (Tatusov et al., 2003) analysis divided homologous genes from different species into different ortholog clusters according to their evolutionary relationship. There were 25 groups of KOG annotations for 8359 *Vm* genes (Fig. S1), of which 2568 genes were annotated as "[S] Function unknown." The top three groups by number of genes were "[G] Carbohydrate transport and metabolism (8.52%)," "[O] Posttranslational modification protein turnover chaperones (6.56%)," and "[Q] Secondary metabolites biosynthesis transport and

catabolism (6.29%).” However, the groups “[W] Extracellular structures (0.05%),” “[N] Cell motility (0.04%),” and “[Y] Nuclear structure (0.04%)” had an insufficient gene quantity.

GO (Gene Ontology) was defined according to the molecular functions, biological pathways, and cytological components of the gene product (Ashburner et al., 2000). Among 11284 gene sequences in the *Vm* genome, 7332 genes had GO annotations, which were classified into 32 categories (Fig. S2). In the class “biological process,” the two most populated categories were “metabolic process” and “cellular process.” In the class “cellular component,” the three most populated categories were “cell,” “cell part,” and “organelle.” In the class “molecular function,” the two most populated categories were “catalytic activity” and “binding.” In contrast, there was only one gene in each of the categories of “cell proliferation,” “locomotion,” “pigmentation,” and “extracellular region part,” respectively.

KEGG (Kyoto Encyclopedia of Genes and Genomes) is a database that systematically analyzes the metabolic pathways of gene products and compounds in cells as well as the function of these gene products (Kanehisa & Goto 2000). There were 3635 genes with KEGG annotations divided into 24 categories (Fig. S3). In addition to the “Global and overview map” category, the seven most populated categories were “Carbohydrate metabolism,” “Amino acid metabolism,” “Translation,” “Signal transduction,” “Transport and catabolism,” and “Cell growth and death.” While the number of genes in the category of “Membrane transport” and “Signaling molecules and interaction” totaled only 0.16% and 0.04% of the genome respectively.

Differential expression analysis and GO, KEGG enrichment analysis

Differentially expressed genes were calculated according to the gene expression count matrix using R package DESeq2. 1476 DEGs with $|\log2FC| \geq 1$ and $P.adj < 0.05$ were obtained from the *Sy* Hhs.015 treatment group compared with the control group, among which 851 genes were up-regulated and 625 genes were down-regulated.A volcano plot was constructed according to gene expression level (Fig. 3). The red dots indicate up-regulated genes, the green dots indicate down-regulated genes and the black dots indicate non-significant differentially expressed genes.

Gene set enrichment analysis was performed to find groups of genes or proteins that are extract over-expressed. GO enrichment analysis was performed to reveal the relationship between the function of DEGs and the response to *Sy* Hhs.015 treatment. The results showed that there were 17 significantly enriched terms ($p.adj < 0.05$) for up-regulated genes (Fig. 4), including “Small molecule metabolic process (GO: 0044281),” “Carboxylic acid metabolic process (GO: 0019752),” “Cellular amino acid metabolic process (GO: 0006520),” “Oxoacid metabolic process (GO: 0043436),” “Organic acid metabolic process (GO: 0006082),” and “Biosynthetic process (GO: 0009058).” Down-regulated genes were significantly enriched in 5 terms ($p.adj < 0.05$) including “Carbohydrate metabolic process (GO: 0005975),” “Transmembrane transport (GO: 0055085),” “Hydrolase activity, acting on glycosyl bonds (GO: 0016798),” “Catalytic activity (GO: 0003824),” “Oxidoreductase activity (GO: 0016491),” and “Hydrolase activity (GO: 0016787).”

KEGG pathway enrichment analysis helps us to analyze gene and expression networks. Pathway enrichment analysis showed that up-regulated genes were significantly enriched in 13

pathways (p.adj < 0.05) (Fig. 5), of which 78 genes were enriched in the "Amino acid metabolism (ko00400, ko00290, ko00300, ko00220, ko00270, ko00250, ko00340, ko00260, ko00360)" pathway. In addition, 18 genes were enriched in the "Translation (ko00970)" pathway and 13 genes were enriched in the "Metabolism of cofactors and vitamins (ko00750, ko00670)" pathway. However, only 3 genes were involved in the pathway "Carbohydrate metabolism (ko00660)." Down-regulated genes were significantly enriched in 15 pathways (p.adj < 0.05), most of which were involved in the "Carbohydrate metabolism (ko00051, ko00040, ko00500, ko00010, ko00630, ko0520, ko00620)" pathway. Pathways related to "Glycan biosynthesis and metabolism (ko00511, ko00513)," "Fatty acid degradation (ko00071)," and "Peroxisome (ko04146)" were also significantly enriched.

Carbohydrate-Active enzymes of DEGs

Carbohydrate-active enzymes (CAZymes) are responsible for the synthesis and metabolism of carbohydrates. CAZymes are often involved in plant pathogens and host interactions (Cantarel et al., 2009). By homology alignment of the CAZy database, 72 Glycoside Hydrolases (GHs), 26 Carbohydrate Esterases (CEs), 7 Carbohydrate-Binding Modules (CBMs), 12 Glycosyl Transferases (GTs) and 24 Auxiliary Activities (AAs) were found in 1476 DEGs (Fig. 6). It is noteworthy that nearly 82% of GH genes were down-regulated, among which 33 of the 40 extracellular enzymes genes were down-regulated (Fig. 7).

qRT-PCR validation

Ten DEGs were selected and qPCR was used to validate the data obtained by differential expression analysis, using G6PDH as an endogenous gene. The qPCR results showed that the actual expression of 10 DEGs was consistent with the trend of gene expression obtained by analysis, but there was a difference in the relative expression level of the genes, which may due to the difference between qPCR technique and the calculation method of differential expression analysis (Fig. 8).

Discussion

In this study, we observed that *Sy* Hhs.015 significantly inhibited the growth of *Vm*. At the subcellular level, the mycelia of *Vm* were distorted and branched. Additionally, we observed extravasation of the protoplasm and the disruption of cellular structure. Comparison of the expression of genes from *Vm* cell that had been inhibited by *Sy* Hhs.015 with that of cells from *Vm* cells, revealed 1476 DEGs.

Our analysis of DEGs revealed that the carbohydrate metabolism of *Vm* had been greatly influenced by *Sy* Hhs.015. In the KOG annotation of DEGs, there were 95 down-regulated genes and 47 up-regulated genes in the group "[G] Carbohydrate transport and metabolism." GO annotation showed that the category "Carbohydrate metabolic process" significantly enriched 62 down-regulated genes (p.adj = 4.55e-14), and the category "hydrolase activity" significantly enriched 85 down-regulated genes (p.adj = 0.0045). The same effect was evident in the large

number of glycoside hydrolase genes that showed down-regulated expression. Pectinase genes (PGs) are key virulence factors for phytopathogenic fungi, which can impair the pectin network of plant cell walls and participate in the maceration of tissues during fungal infection (Hoondal et al., 2002). Three PGs (KUI67703.1, KUI69548.1, KUI73936.1) among the DEGs were down-regulated, which may affect *Vm* infectivity. Carbohydrate metabolism is an important way for the organism to gain energy (Kandler 1983). Heterotrophic fungi, for example, usually gain nutrients by secreting extracellular hydrolase. The hydrolases secreted by pathogenic fungi can damage plant cell wall by breaking down polysaccharides, thereby facilitating infection (Paccanaro et al., 2017). We found that *Sy* Hhs.015 can affect the carbohydrate metabolic pathway of *Vm*, reducing its ability to gain energy, thereby inhibiting its growth, and potentially reducing the pathogenicity of its infection.

Chitin, dextran and various proteins are important components of the fungal cell wall (Bowman & Free 2006). Interestingly, four of the five genes associated with cell walls in DEGs were down-regulated, while eight down-regulated genes appeared in the "Glycan biosynthesis and metabolism" pathway. One Chitin deacetylase 1 gene (KUI65489.1) that played a role in cell wall chitosan biosynthesis was also down-regulated (log2FC = -2.42) (GaoKatsumoto & Onodera 1995). It could be inferred that the ability to biosynthesize the polysaccharide components in the cell wall had decreased. Chitinase is an important enzyme that degrades cell compartments and achieves cell separation during fungal proliferation (Merzendorfer & Zimoch 2003). Two Chitinase 1 genes (KUI66287.1, KUI69708.1) among the DEGs were significantly down-regulated (log2FC = -2.21). Meanwhile, chitinase, proteinase and glucanase produced by *Sy* Hhs.015 also destroyed the cell wall structure of *Vm* (Fan et al., 2016). Combining these factors, it can be speculated that *Sy* Hhs.015 damaged the cell wall of *Vm* and cell wall formation and cell division were blocked, resulting in the inhibition of *Vm* growth.

Peroxisomes are a type of monolayer organelle commonly found in eukaryotes, and contain oxidase, catalase, and peroxidase (De Duve & Baudhuin 1966). Catalase is a peroxidase marker enzyme, and its main function is to hydrolyze the cytotoxic substance H_2O_2 produced in oxidase catalyzed redox reactions. Seven down-regulated genes were significantly enriched in the "Peroxidase" pathway (p.adj=0.0196), including a catalase gene (KUI65198.1, log2FC = -2.29) and a superoxide dismutase gene (KUI66682.1, log2FC = -1.19). These changes may not only affect the oxidation of toxic substances such as formic acid and phenol, but also accumulate H_2O_2, leading to cell damage. The pathogen's fungal glyoxylate cycle are involved in its infection process (Lorenz & Fink 2001). Malic acid synthase (MS) and Isocitrate lyase (ICL) are the key enzymes in the glyoxylate cycle, both of which are also present in the peroxisome. Down-regulation of the two genes may reduce the succinic acid intermediate product of glyoxylate cycle required for the TCA cycle, allowing *Vm* to gain more energy. Medium-chain fatty acids produced by the beta-oxidation of fatty acids affect the production of pigments and toxins in fungi. In addition, acetyl coenzyme A, another product, is both essential for the infection process and promotes gluconeogenesis (Wang et al., 2007). Two down-regulated genes (KUI71646.1, "alpha-methylacyl-CoA racemase," log2FC = -1.34; KUI64199.1, "acetyl-CoA acyltransferase 1," log2FC = -1.15) of β-oxidation related to fatty acid may affect the fatty acid metabolism and the

pathogenicity of *Vm*.

Organisms can respond to external stress through their own regulation mechanisms (Rowley et al., 2006). The pathways "Amino acid metabolism (78 up-regulated genes)" and "Aminoacyl-tRNA biosynthesis (18 up-regulated genes)," that are related to translation and involved in amino acid biosynthesis, were significantly enriched (Ibba & Söll 2000). The pathway "Vitamin B6 metabolism (6 up-regulated genes)" was also enriched. Vitamin B 6 can participate in amino acid, glucose, and lipid metabolism via its metabolically active form, pyridoxal 5'-phosphate (PLP) (Ink & Henderson 1984). Furthermore, the KOG annotation also showed that amino acid biosynthesis and metabolism had been enhanced, including the groups "[O] Posttranslational modification protein turnover chaperones (36 up-regulated, 18 down-regulated)" and "[E] Amino acid transport and metabolism (68 up-regulated,29 down-regulated)." The amino acid biosynthesis and metabolism pathways have two beneficial purposes: the synthesis of the proteins needed for survival and the generation of α-keto acids, through deamination and transamination, which can then participate in carbohydrate metabolism, lipid metabolism and the TCA cycle to obtain energy. For instance, glutamate generates α-ketoglutaric acid, involved in TCA cycle, which is catalyzed by glutamate dehydrogenase (Sugden & Newsholme 1975), and can compensate for a lack of carbohydrate metabolism. Four retinol dehydrogenase genes were up-regulated: these are associated with dextran synthesis (Meaden et al., 1990) and may be involved in the stress repair process after the cell wall destruction of *Vm*. Ergosterol is an important component of the cell membrane, and interestingly, we found that the sterol 24-C-methyltransferase gene involved in its synthesis was up-regulated (Ahmad et al., 2011; Ganapathy et al., 2011). Glutathione S-transferase (GST) functions in the processes of detoxification and anti-oxidation and can also catalyze the binding of GSH^- to electrophilic centers on toxic substrates through sulfhydryl groups. Likewise, ABC transporters have the efflux function of excreting toxic substances (Meyer et al., 2007). Two GST genes (KUI68053.1, KUI73914.1) and two ABC transporters genes (KUI66519.1, KUI68518.1) were up-regulated, which most likely contributed to the detoxification and anti-oxidation of *Vm*. We also found that the Streptothricin hydrolase gene (KUI73345.1, log2FC = 3.38) was significantly up-regulated, which might indicate a counter response of *Vm* to antimicrobial substances such as antibiotics produced by *Sy* Hhs.015.

Conclusion

In conclusion, we have shed light on the response mechanism of *Vm* to *Sy* Hhs.015 (Fig. 9). A variety of antimicrobial substances produced by *Sy* Hhs.015 affected the carbohydrate metabolism of *Vm* the main energy production pathway. The cell wall and membrane structure of *Vm* was also destroyed, affecting its peroxisomal function, and leading to reduce output of toxic substances, which could lead to a reduction in pathogenicity. *Vm* also enhanced its metabolism of amino acids to synthesize its own nitrogen-containing substances and gain energy through the production of alpha-keto acids involved in carbohydrate metabolism, lipid metabolism and TCA cycle. We also observed up-regulation of the expression of retinol dehydrogenase genes involved in dextran biosynthesis as well as the sterol 24-C-methyltransferase gene, which are involved in

the synthesis and repair of cell walls and cell membranes. Additionally, the GST and ABC transporter genes were up-regulated to increase antioxidant function and the ability of *Vm* to excrete extracellular substances. We also speculate that *Vm* could to some extent degrade the antimicrobial substances produced by *Sy* Hhs.015. Overall, the results of this research provide a theoretical basis for clarifying the biological control mechanism of *Sy* Hhs.015 and the response mechanism of *Vm* to stress.

References

Ahmad A, Khan A, Akhtar F, Yousuf S, Xess I, Khan LA, and Manzoor N. 2011. Fungicidal activity of thymol and carvacrol by disrupting ergosterol biosynthesis and membrane integrity against Candida. *Eur J Clin Microbiol Infect Dis* 30:41-50. DOI:10.1007/s10096-010-1050-8

Anders S, Pyl PT, and Huber W. 2015. HTSeq--a Python framework to work with high-throughput sequencing data. *Bioinformatics* 31:166-169. DOI:10.1093/bioinformatics/btu638

Arocho A, Chen B, Ladanyi M, and Pan Q. 2006. Validation of the 2-ΔΔCt Calculation as an Alternate Method of Data Analysis for Quantitative PCR of BCR-ABL P210 Transcripts. *Diagnostic Molecular Pathology* 15:56-61.

Ashburner M, Ball CA, Blake JA, Botstein D, Butler H, Cherry JM, Davis AP, Dolinski K, Dwight SS, Eppig JT, Harris MA, Hill DP, Issel-Tarver L, Kasarskis A, Lewis S, Matese JC, Richardson JE, Ringwald M, Rubin GM, and Sherlock G. 2000. Gene ontology: tool for the unification of biology. The Gene Ontology Consortium. *Nat Genet* 25:25-29. DOI:10.1038/75556

Biggs AR. 1990. Managing wound-associated diseases by understanding wound healing in the bark of woody plants. *Journal of Arboriculture* 16:109.

Bolger AM, Lohse M, and Usadel B. 2014. Trimmomatic: a flexible trimmer for Illumina sequence data. *Bioinformatics* 30:2114-2120. DOI:10.1093/bioinformatics/btu170

Bowman SM, and Free SJ. 2006. The structure and synthesis of the fungal cell wall. *Bioessays* 28:799-808. DOI:10.1002/bies.20441

Cantarel BL, Coutinho PM, Rancurel C, Bernard T, Lombard V, and Henrissat B. 2009. The Carbohydrate-Active EnZymes database (CAZy): an expert resource for Glycogenomics. *Nucleic Acids Res* 37:D233-238. DOI:10.1093/nar/gkn663

Cao K, Guo L, Li B, Sun G, and Chen H. 2009. Investigations on the occurrence and control of apple canker in China. *Plant Protection* 25:384-389.

Castillo UF, Strobel GA, Ford EJ, Hess WM, Porter H, Jensen JB, Albert H, Robison R, Condron MA, Teplow DB, Stevens D, and Yaver D. 2002. Munumbicins, wide-spectrum antibiotics produced by Streptomyces NRRL 30562, endophytic on Kennedia nigriscans. *Microbiology* 148:2675-2685. DOI:10.1099/00221287-148-9-2675

Compant S, Duffy B, Nowak J, Clement C, and Barka EA. 2005. Use of plant growth-promoting bacteria for biocontrol of plant diseases: principles, mechanisms of action, and future prospects. *Appl Environ Microbiol* 71:4951-4959. DOI:10.1128/aem.71.9.4951-

4959.2005
Conesa A, Gotz S, Garcia-Gomez JM, Terol J, Talon M, and Robles M. 2005. Blast2GO: a universal tool for annotation, visualization and analysis in functional genomics research. *Bioinformatics* 21:3674-3676. DOI:10.1093/bioinformatics/bti610
Database Resources of the BIG Data Center in 2018. Nucleic Acids Res 46:D14-d20. DOI:10.1093/nar/gkx897
De Duve C, and Baudhuin P. 1966. Peroxisomes (microbodies and related particles). *Physiological reviews* 46:323-357.
Fan D, Li Y, Zhao L, Li Z, Huang L, and Yan X. 2016. Study on Interactions between the Major Apple Valsa Canker Pathogen Valsa mali and Its Biocontrol Agent Saccharothrix yanglingensis Hhs.015 Using RT-qPCR. *PLoS One* 11:e0162174. DOI:10.1371/journal.pone.0162174
Ganapathy K, Kanagasabai R, Nguyen TT, and Nes WD. 2011. Purification, characterization and inhibition of sterol C24-methyltransferase from Candida albicans. *Arch Biochem Biophys* 505:194-201. DOI:10.1016/j.abb.2010.10.008
Gao XD, Katsumoto T, and Onodera K. 1995. Purification and characterization of chitin deacetylase from Absidia coerulea. *J Biochem* 117:257-263. DOI:10.1093/jb/117.2.257
Hoondal GS, Tiwari RP, Tewari R, Dahiya N, and Beg QK. 2002. Microbial alkaline pectinases and their industrial applications: a review. *Appl Microbiol Biotechnol* 59:409-418. DOI:10.1007/s00253-002-1061-1
Ibba M, and Söll D. 2000. Aminoacyl-tRNA synthesis. *Annual review of biochemistry* 69:617-650.
Ink SL, and Henderson LM. 1984. Vitamin B6 metabolism. *Annual review of nutrition* 4:455-470.
Kandler O. 1983. Carbohydrate metabolism in lactic acid bacteria. *Antonie Van Leeuwenhoek* 49:209-224.
Kanehisa M, and Goto S. 2000. KEGG: kyoto encyclopedia of genes and genomes. *Nucleic acids research* 28:27-30. DOI: 10.1093/nar/28.1.27
Ke X, Yin Z, Song N, Dai Q, Voegele RT, Liu Y, Wang H, Gao X, Kang Z, and Huang L. 2014. Transcriptome profiling to identify genes involved in pathogenicity of Valsa mali on apple tree. *Fungal Genet Biol* 68:31-38. DOI:10.1016/j.fgb.2014.04.004
Kim D, Langmead B, and Salzberg SL. 2015. HISAT: a fast spliced aligner with low memory requirements. *Nat Methods* 12:357-360. DOI:10.1038/nmeth.3317
Li Z, Gao X, Kang Z, Huang L, Fan D, Yan X, and Kang Z. 2016. Saccharothrix yanglingensis strain Hhs. 015 is a promising biocontrol agent on apple valsa canker. *Plant Disease* 100:510-514. DOI:10.1094/PDIS-02-15-0190-RE
Lorenz MC, and Fink GR. 2001. The glyoxylate cycle is required for fungal virulence. *Nature* 412:83-86. DOI:10.1038/35083594
Love MI, Huber W, and Anders S. 2014. Moderated estimation of fold change and dispersion for RNA-seq data with DESeq2. *Genome Biol* 15:550. DOI:10.1186/s13059-014-0550-8
Meaden P, Hill K, Wagner J, Slipetz D, Sommer SS, and Bussey H. 1990. The yeast KRE5 gene encodes a probable endoplasmic reticulum protein required for (1----6)-beta-D-glucan

425 synthesis and normal cell growth. *Mol Cell Biol* 10:3013-3019.
426 DOI:10.1128/MCB.10.6.3013
427 Merzendorfer H, and Zimoch L. 2003. Chitin metabolism in insects: structure, function and
428 regulation of chitin synthases and chitinases. *J Exp Biol* 206:4393-4412.
429 DOI:10.1242/jeb.00709
430 Meyer V, Damveld RA, Arentshorst M, Stahl U, van den Hondel CA, and Ram AF. 2007. Survival
431 in the presence of antifungals: genome-wide expression profiling of Aspergillus niger in
432 response to sublethal concentrations of caspofungin and fenpropimorph. *J Biol Chem*
433 282:32935-32948. DOI:10.1074/jbc.M705856200
434 Miles L, Lopera C, González S, de García MC, Franco A, and Restrepo S. 2012. Exploring the
435 biocontrol potential of fungal endophytes from an Andean Colombian Paramo ecosystem.
436 *BioControl* 57:697-710. DOI:10.1007/s10526-012-9442-6
437 Paccanaro MC, Sella L, Castiglioni C, Giacomello F, Martinez-Rocha AL, D'Ovidio R, Schafer
438 W, and Favaron F. 2017. Synergistic Effect of Different Plant Cell Wall-Degrading
439 Enzymes Is Important for Virulence of Fusarium graminearum. *Mol Plant Microbe*
440 *Interact* 30:886-895. DOI:10.1094/mpmi-07-17-0179-r
441 Qin S, Xing K, Jiang JH, Xu LH, and Li WJ. 2011. Biodiversity, bioactive natural products and
442 biotechnological potential of plant-associated endophytic actinobacteria. *Appl Microbiol*
443 *Biotechnol* 89:457-473. DOI:10.1007/s00253-010-2923-6
444 Rowley G, Spector M, Kormanec J, and Roberts M. 2006. Pushing the envelope: extracytoplasmic
445 stress responses in bacterial pathogens. *Nature Reviews Microbiology* 4:383.
446 DOI:10.1038/nrmicro1394
447 Subramanian A, Tamayo P, Mootha VK, Mukherjee S, Ebert BL, Gillette MA, Paulovich A,
448 Pomeroy SL, Golub TR, Lander ES, and Mesirov JP. 2005. Gene set enrichment analysis:
449 a knowledge-based approach for interpreting genome-wide expression profiles. *Proc Natl*
450 *Acad Sci U S A* 102:15545-15550. DOI:10.1073/pnas.0506580102
451 Sugden P, and Newsholme E. 1975. Activities of citrate synthase, NAD+-linked and NADP+-
452 linked isocitrate dehydrogenases, glutamate dehydrogenase, aspartate aminotransferase
453 and alanine aminotransferase in nervous tissues from vertebrates and invertebrates.
454 *Biochemical Journal* 150:105-111. DOI:10.1042/bj1500105
455 Tatusov RL, Fedorova ND, Jackson JD, Jacobs AR, Kiryutin B, Koonin EV, Krylov DM,
456 Mazumder R, Mekhedov SL, Nikolskaya AN, Rao BS, Smirnov S, Sverdlov AV,
457 Vasudevan S, Wolf YI, Yin JJ, and Natale DA. 2003. The COG database: an updated
458 version includes eukaryotes. *BMC Bioinformatics* 4:41. DOI:10.1186/1471-2105-4-41
459 Wang C, Li C, Li B, Li G, Dong X, Wang G, and Zhang Q. 2014a. Toxins produced by Valsa mali
460 var. mali and their relationship with pathogenicity. *Toxins (Basel)* 6:1139-1154.
461 DOI:10.3390/toxins6031139
462 Wang X, Zang R, Yin Z, Kang Z, and Huang L. 2014b. Delimiting cryptic pathogen species
463 causing apple Valsa canker with multilocus data. *Ecol Evol* 4:1369-1380.
464 DOI:10.1002/ece3.1030
465 Wang Y, Song F, Zhu J, Zhang S, Yang Y, Chen T, Tang B, Dong L, Ding N, Zhang Q, Bai Z,

Dong X, Chen H, Sun M, Zhai S, Sun Y, Yu L, Lan L, Xiao J, Fang X, Lei H, Zhang Z, and Zhao W. 2017. GSA: Genome Sequence Archive(). Genomics Proteomics Bioinformatics 15:14-18. DOI:10.1016/j.gpb.2017.01.001

Wang ZY, Soanes DM, Kershaw MJ, and Talbot NJ. 2007. Functional analysis of lipid metabolism in Magnaporthe grisea reveals a requirement for peroxisomal fatty acid beta-oxidation during appressorium-mediated plant infection. *Mol Plant Microbe Interact* 20:475-491. DOI:10.1094/mpmi-20-5-0475

Yan X, Huang LL, Tu X, Gao XN, and Kang ZS. 2012. Saccharothrix yanglingensis sp. nov., an antagonistic endophytic actinomycete isolated from cucumber plant. *Antonie Van Leeuwenhoek* 101:141-146. DOI:10.1007/s10482-011-9631-9

Yin Z, Liu H, Li Z, Ke X, Dou D, Gao X, Song N, Dai Q, Wu Y, Xu JR, Kang Z, and Huang L. 2015. Genome sequence of Valsa canker pathogens uncovers a potential adaptation of colonization of woody bark. *New Phytol* 208:1202-1216. DOI:10.1111/nph.13544

Figure 1(on next page)

Schematic diagram of *Sy* Hhs.015 inhibiting *Vm* in the petri dish.

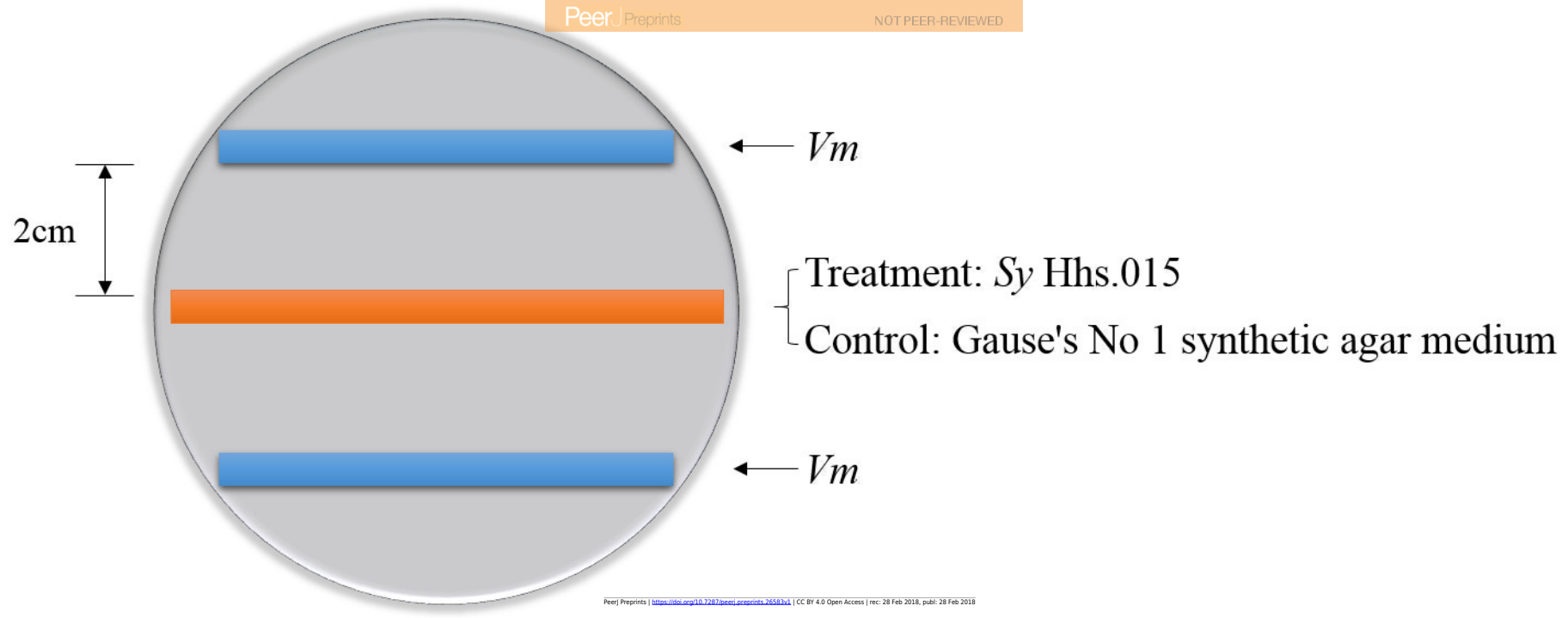

Figure 2(on next page)

Graphs of *Vm* treated with *Sy* Hhs.015 for 48 hours.

(A) Normal growth of *Vm*. (B) *Vm* treated with *Sy* Hhs.015.

Mycelial morphology observed by optical microscope, bar=10 μm: (C) Normal hyphae. (D) Abnormal hyphae with branches.

Subcellular structure of mycelium observed by transmission electron microscope, bar=500 nm: (E) Normal *Vm* showed a clear and complete cell structure. (F) Treated *Vm* showed thickening of cell walls and organelle degradation.

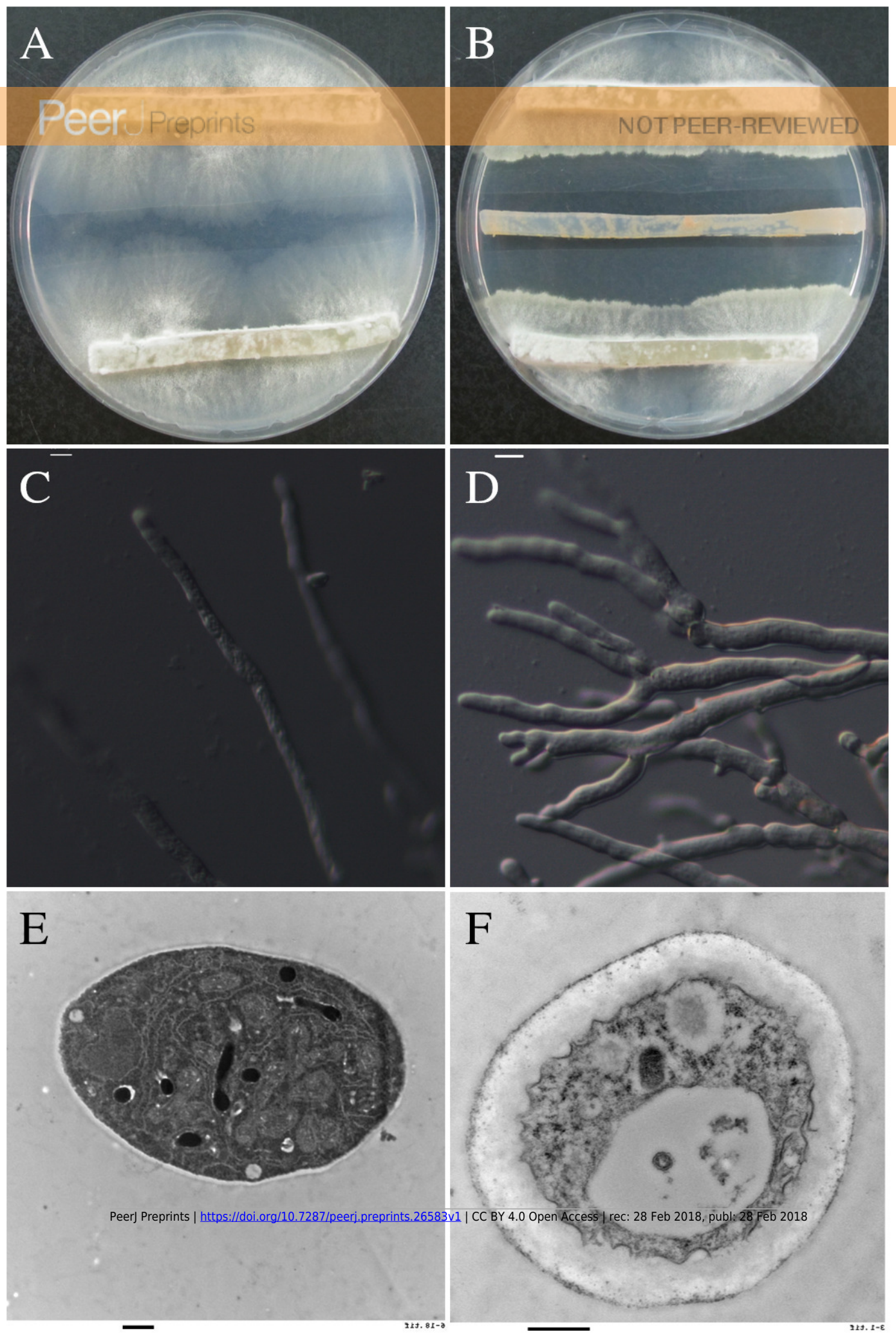

PeerJ Preprints | https://doi.org/10.7287/peerj.preprints.26583v1 | CC BY 4.0 Open Access | rec: 28 Feb 2018, publ: 28 Feb 2018

Figure 3(on next page)

Volcano plot of DEGs between *Sy* Hhs.015 treatment group and control group.

The red dots indicate up-regulated genes, the green dots indicate down-regulated genes and the black dots indicate non-significant differentially expressed genes.

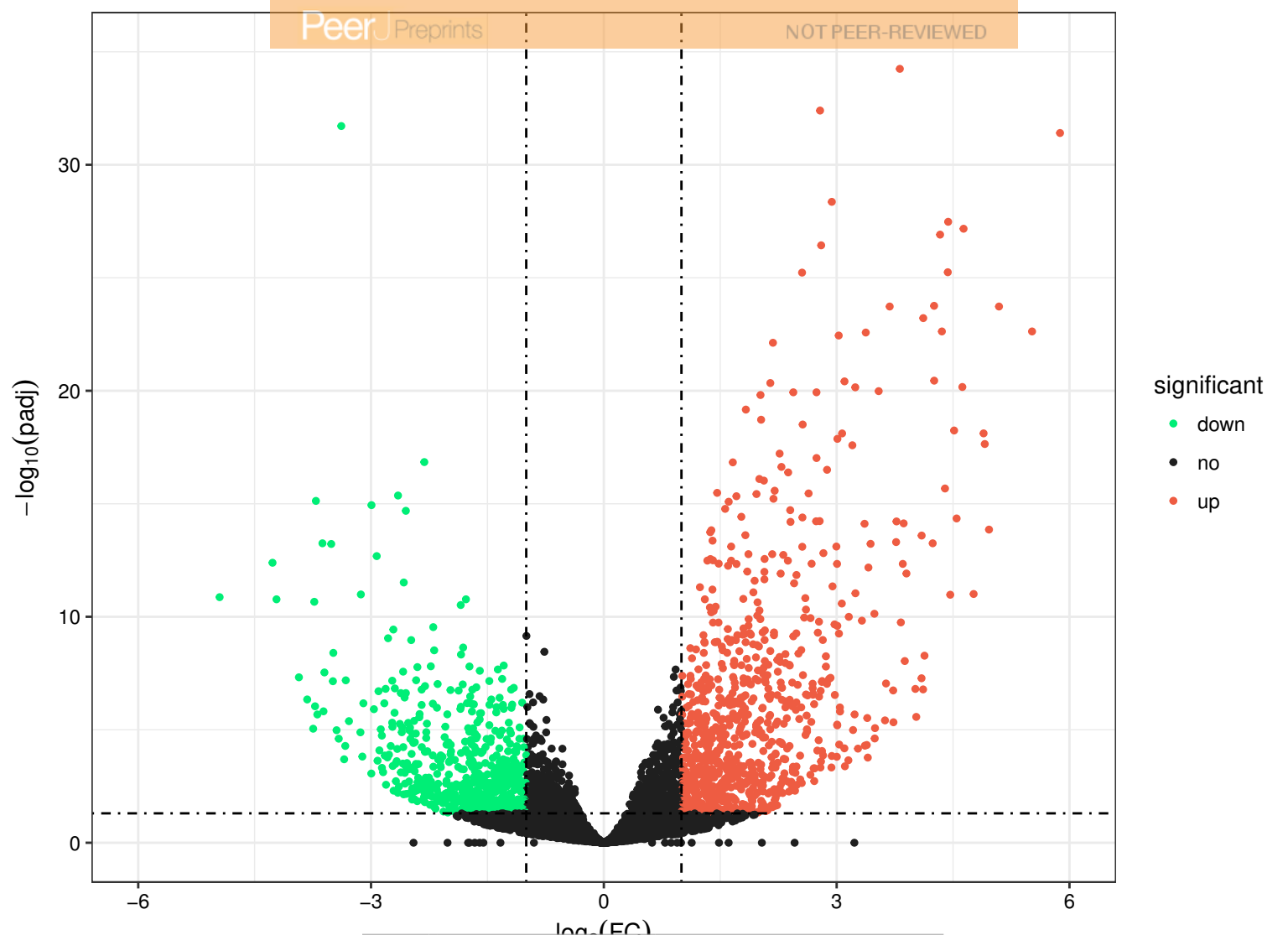

PeerJ Preprints | https://doi.org/10.7287/peerj.preprints.26393v1 | CC BY 4.0 Open Access | rec: 28 Feb 2018, publ: 28 Feb 2018

Figure 4(on next page)

Bar plot of GO enrichment analysis of DEGs.

'Count' indicates the number of DEGs enriched in GO term. And 'p.adj' indicates the p-value corrected by 'BH' method.

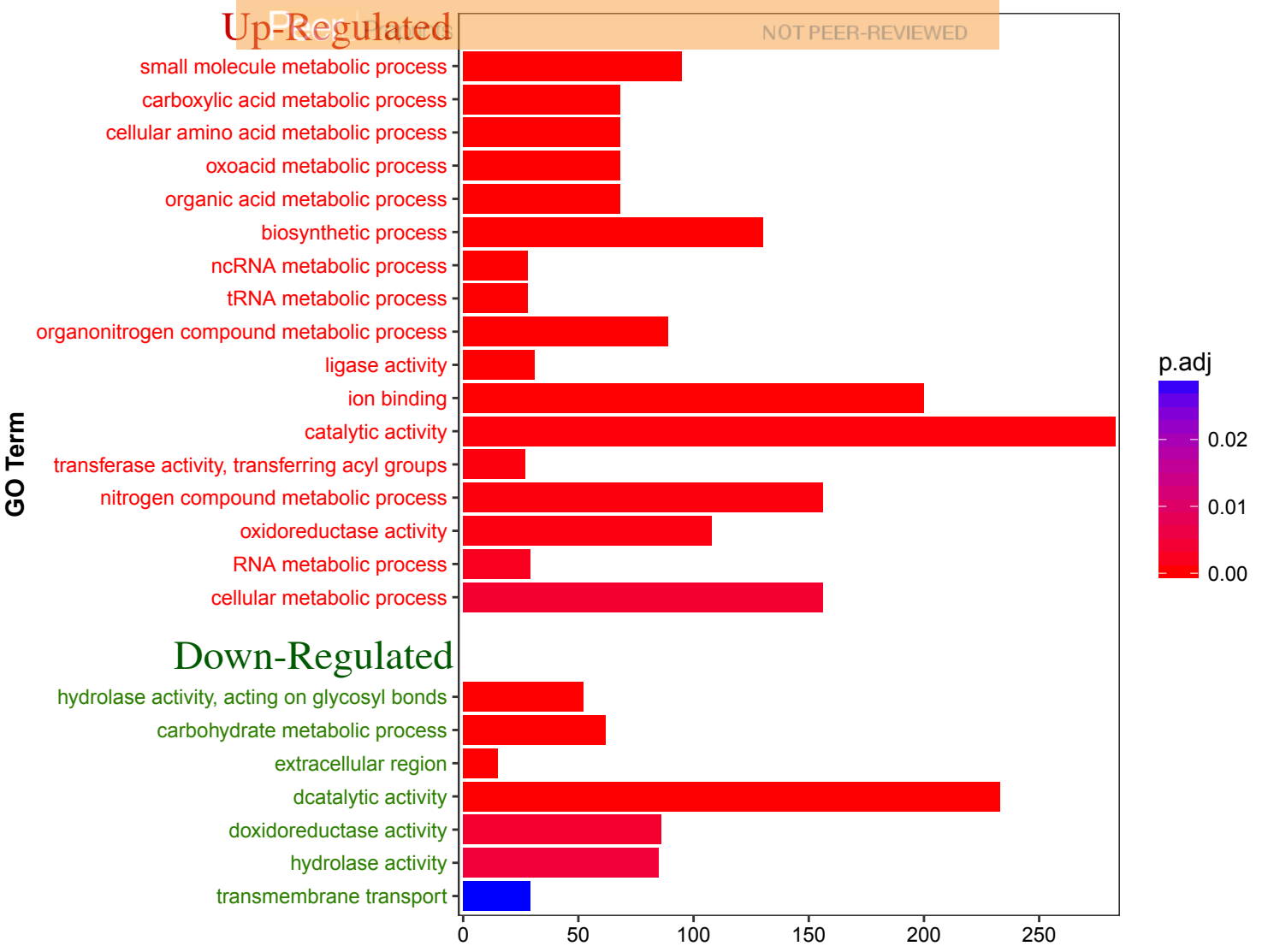

PeerJ Preprints | https://doi.org/10.7287/peerj.preprints.26583v1 | CC BY 4.0 Open Access | rec: 28 Feb 2018, publ: 28 Feb 2018

Figure 5(on next page)

Bubble plot of KEGG pathway enrichment analysis of DEGs.

'Count' indicates the number of DEGs enriched in pathway. 'GeneRatio' indicates the ratio of enriched DEGs to background genes. And 'p.adj' indicates the p-value corrected by 'BH' method.

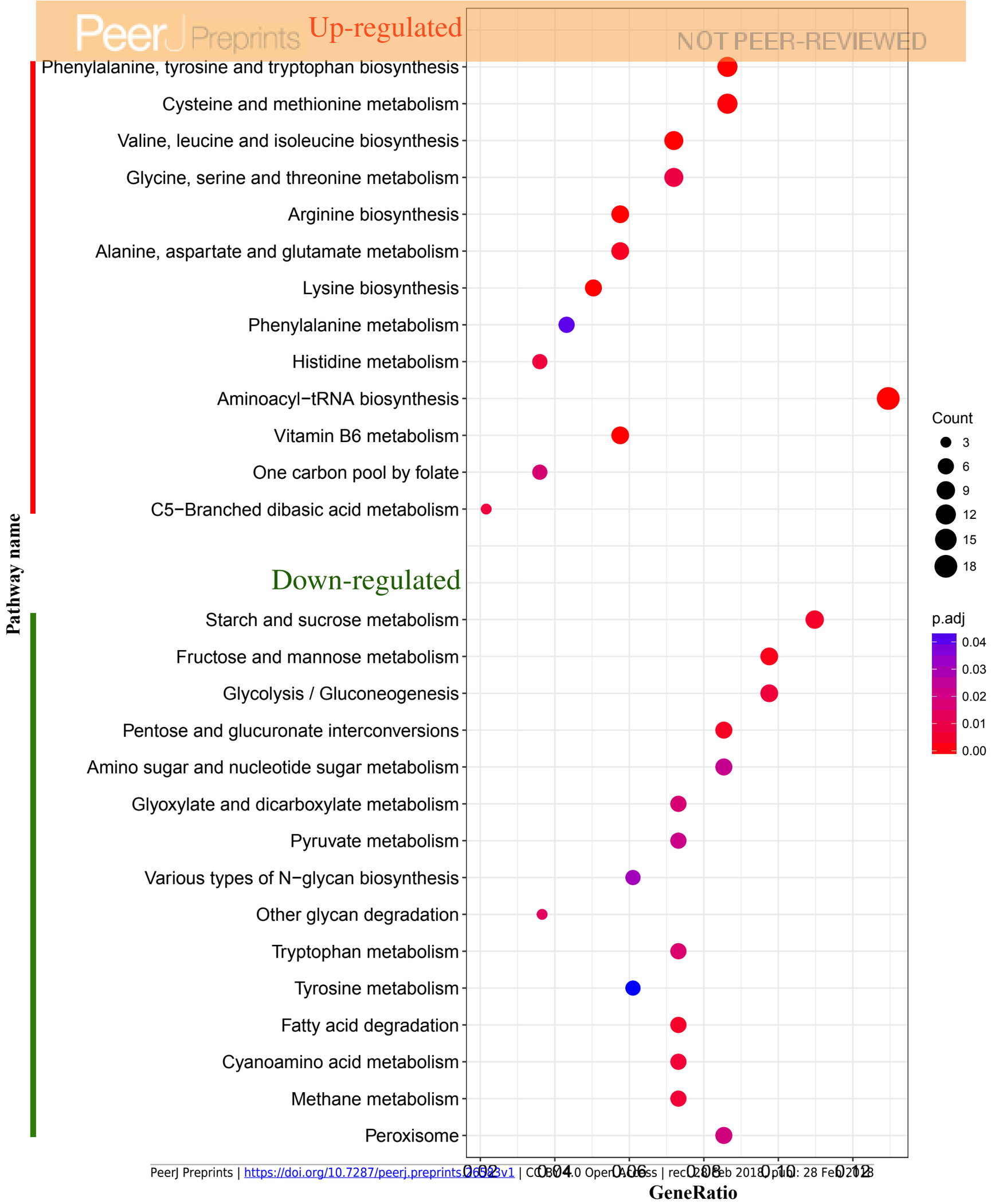

Figure 6

Statistics of up-regulated and down-regulated CAZy in DEGs.

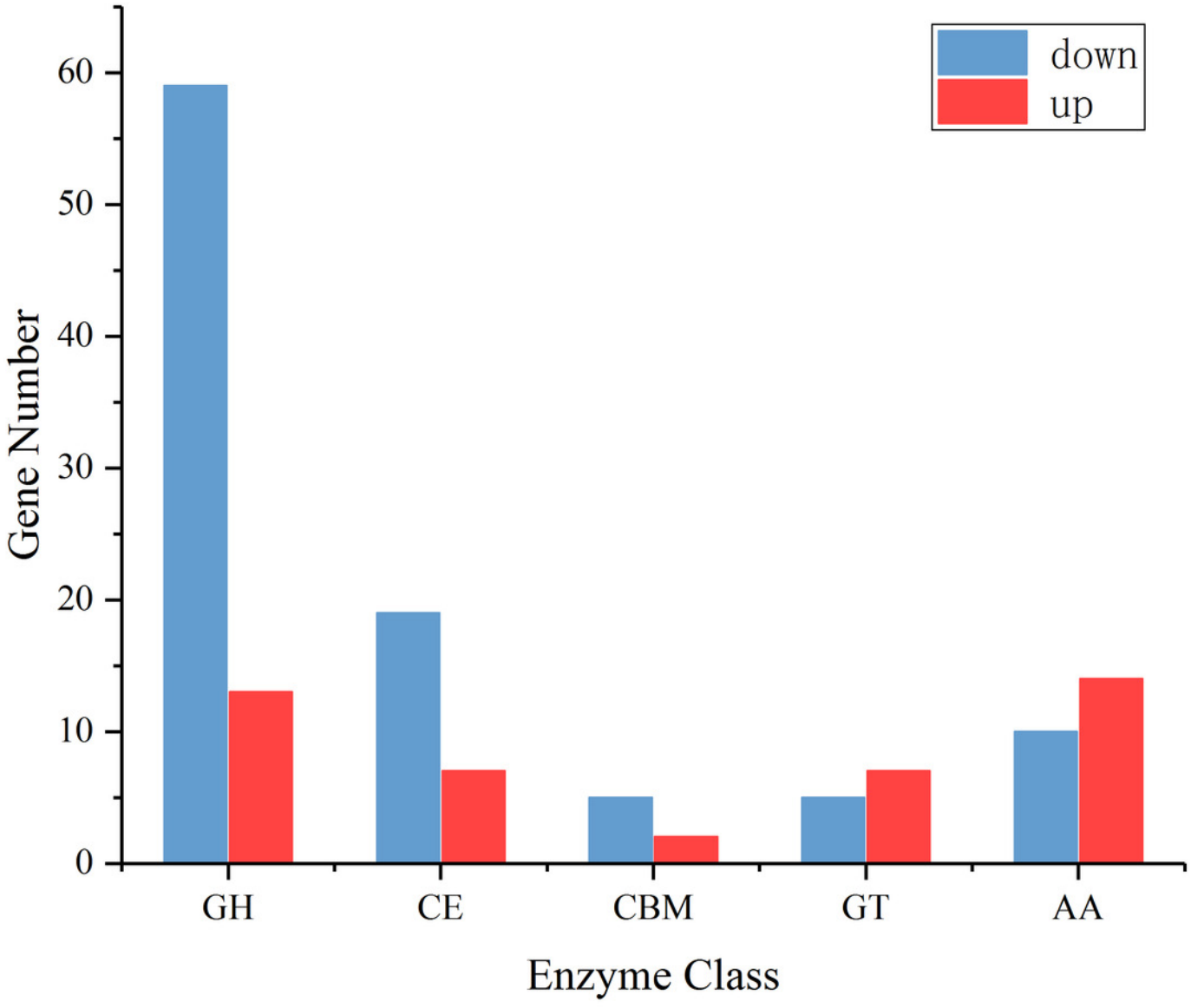

Figure 7 (on next page)

Heatmap of extracellular glycosyl hydrolases.

The color scale indicates the counts of gene expression normalized by Z-score.

PeerJ Preprints | https://doi.org/10.7287/peerj.preprints.26583v1 | CC BY 4.0 Open Access | rec: 28 Feb 2018, publ: 28 Feb 2018

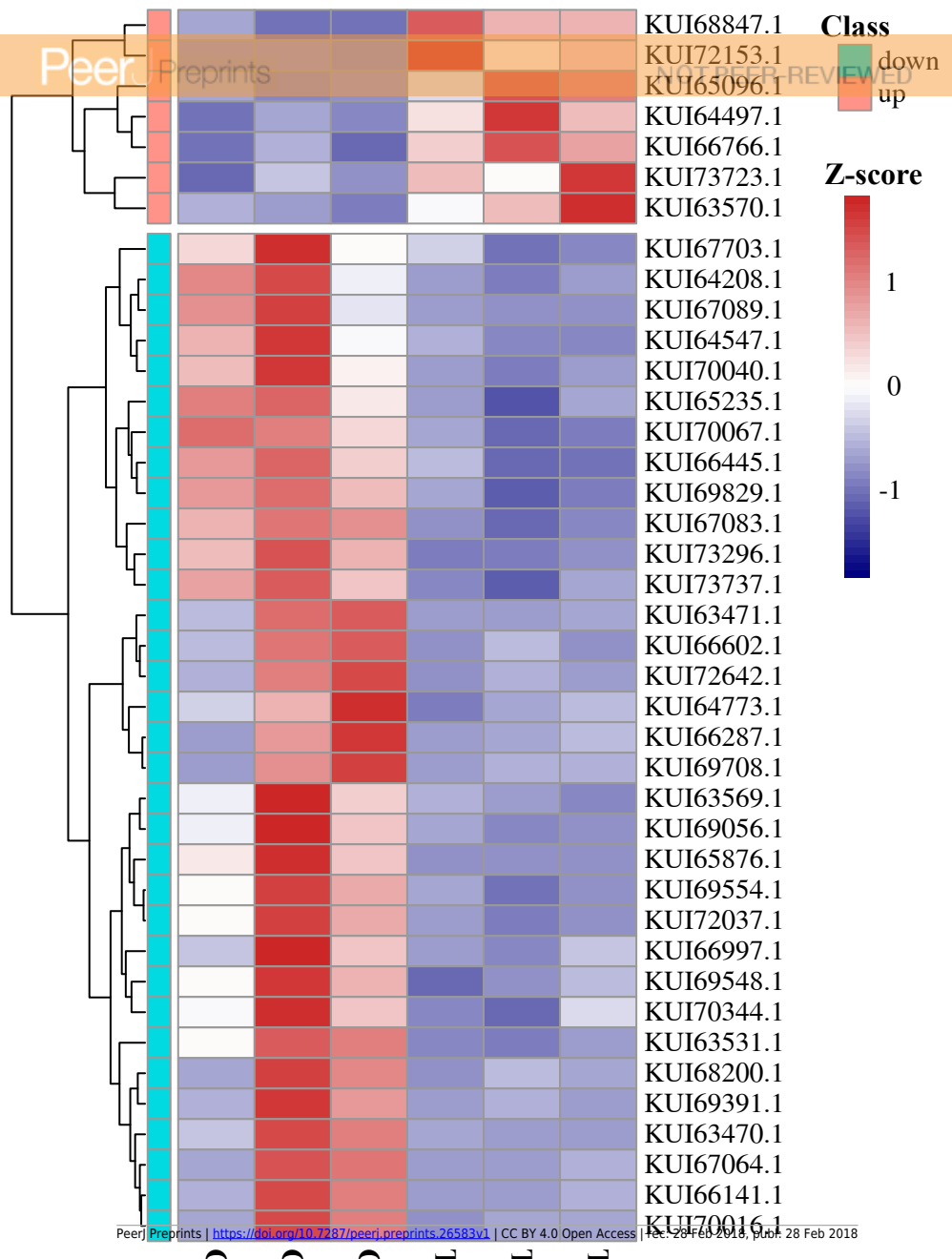

PeerJ Preprints | https://doi.org/10.7287/peerj.preprints.26583v1 | CC BY 4.0 Open Access | rec: 28 Feb 2018, pub: 28 Feb 2018

Figure 8

Relative expression level of fourteen DEGs using reference gene G6PDH for normalization.

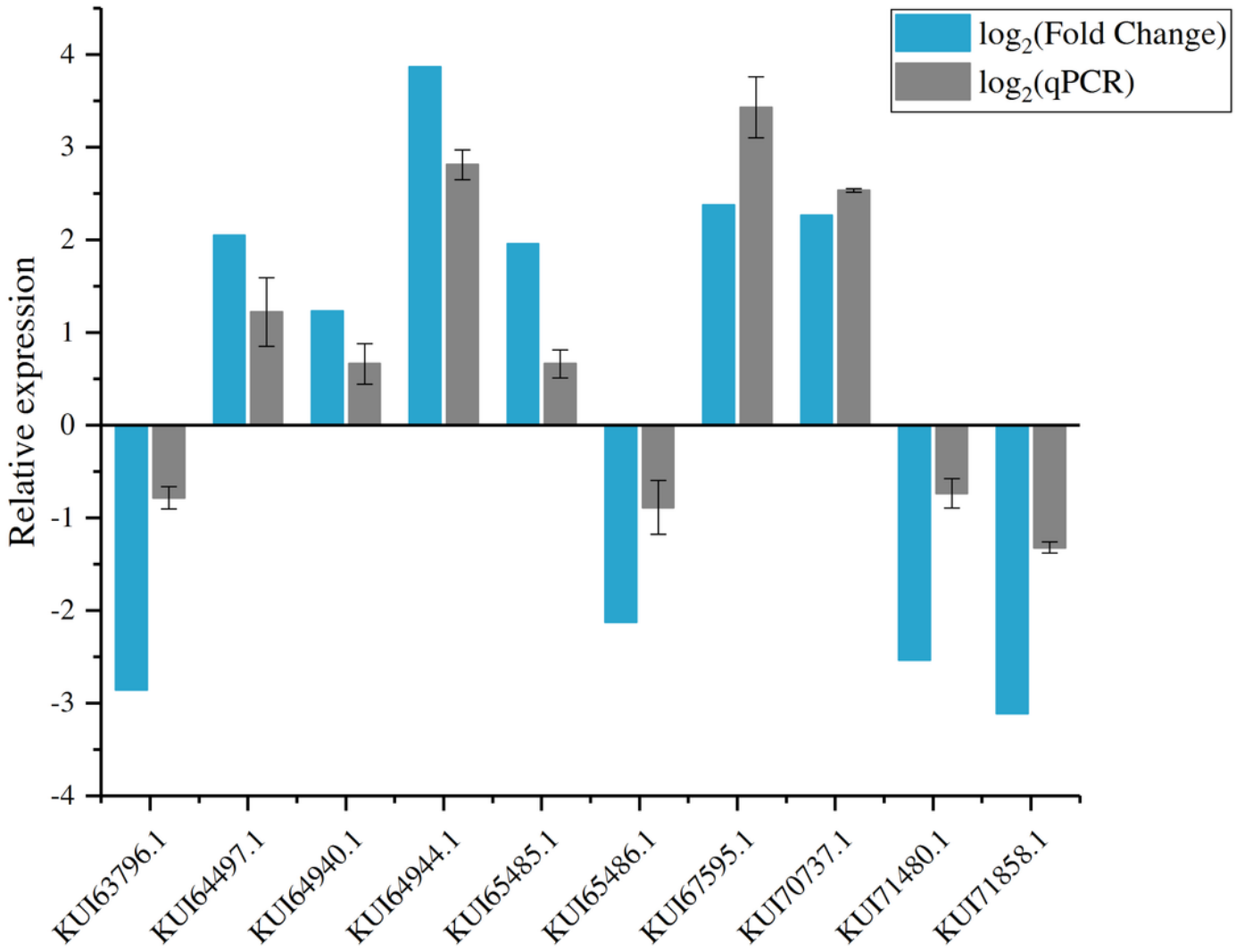

Figure 9

The mode diagram of Vm response to Sy Hhs.015.

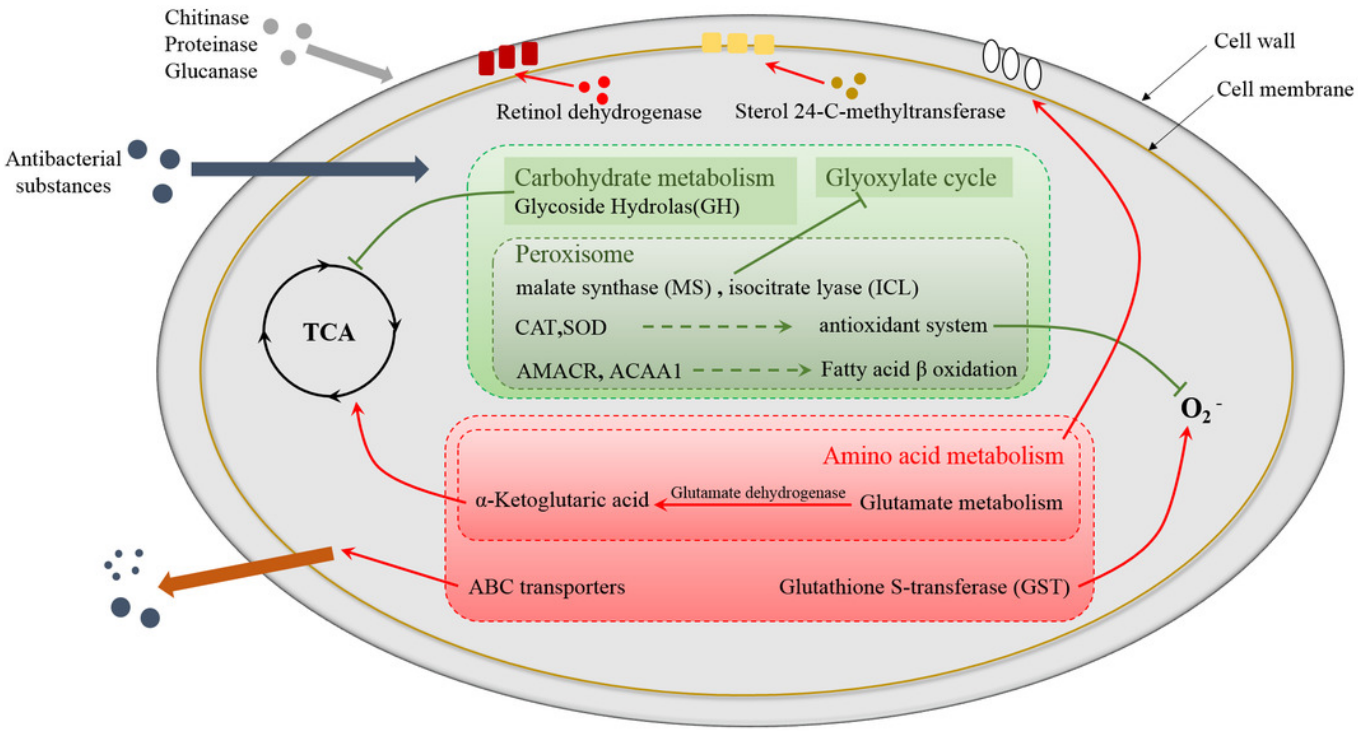

Table 1(on next page)

Primers used in qRT-PCR.

Gene ID			Primers	
KUI63796.1	F:	5’	ACGCCTATCAGTACCGTCCACA	3'
	R:	5’	TTGCCGTTATACACGTCCCAC	3'
KUI64497.1	F:	5’	GACTGGTCACTTCCCCTAACTTCA	3'
	R:	5’	TTTCGTCCACGGGCTTCTT	3'
KUI64940.1	F:	5’	GCCGTCCTTTCGAACTCTATC	3'
	R:	5’	ACTGGTCGAGACCTTCATCT	3'
KUI64944.1	F:	5’	CGAGTTCTACCAGTGCGATTT	3'
	R:	5’	CGAGAAGCCCTCGACAATAATC	3'
KUI65485.1	F:	5’	TGGGTTTCATCTGAGCCATAC	3'
	R:	5’	CATAGGCAGTGGGCTGTATAAT	3'
KUI65486.1	F:	5’	CGTGGGGTTATACCAGAAAGACA	3'
	R:	5’	TCGGAGACGCCGTAGTAAAGAC	3'
KUI67595.1	F:	5’	AGGTGTTTCACAAAGGTCTGCC	3'
	R:	5’	CGACTGCCCTTACTGAACGATAT	3'
KUI70737.1	F:	5’	GAGCCTTCTCAGAGCTTCAAT	3'
	R:	5’	GTGTTCCATAAGTCCTCCTTCTC	3'
KUI71480.1	F:	5’	CGCTTGAGGAGCTGGATATTT	3'
	R:	5’	CACCAAGCCCAAAGTCTGATA	3'
KUI71858.1	F:	5’	CGTACTGCCGTCTTGCTAAA	3'
	R:	5’	CGTCATCTGTGTCCTCCAATC	3'

PeerJ Preprints | https://doi.org/10.7287/peerj.preprints.26583v1 | CC BY 4.0 Open Access | rec: 28 Feb 2018, publ: 28 Feb 2018

Table 2(on next page)

Statistics of sequencing production and mapping ratio.

Sample	Raw reads	Clean reads	Clean bases	Q30(%)	GC(%)	Total mapped Ratio (%)
C1_1	11645164	10899898	1.36G	92.45	55.84	96.89
C1_2	11645164	10899898	1.36G	89.78	55.82	
C2_1	10609958	10166658	1.27G	92.22	55.05	96.97
C2_2	10609958	10166658	1.27G	89.50	55.03	
C3_1	10455527	9917147	1.24G	92.70	55.04	96.79
C3_2	10455527	9917147	1.24G	89.06	55.02	
T1_1	10848694	10403574	1.30G	93.49	55.35	96.56
T1_2	10848694	10403574	1.30G	91.03	55.37	
T2_1	11187720	10767189	1.35G	93.54	55.12	96.65
T2_2	11187720	10767189	1.35G	90.88	55.13	
T3_1	11845541	11311637	1.41G	92.72	55.19	96.47
T3_2	11845541	11311637	1.41G	89.50	55.16	